Mathematical Models and Methods in Applied Sciences
Vol. 10, No. 7 (2000) 1099–1120

NUMERICAL SOLUTION FOR HYDRODYNAMICAL MODELS OF SEMICONDUCTORS

VITTORIO ROMANO*
Dipartimento Interuniversitario di Matematica, Politecnico di Bari, via E.Orabona 4-70125 Bari, Italy

GIOVANNI RUSSO†
Dipartimento di Matematica, Università dell'Aquila, Via Vetoio, loc. Coppito-67100 L'Aquila, Italy

Communicated by P. A. Markowich
Received 23 November 1998
Revised 14 June 1999

Numerical solutions of recent hydrodynamical models of semiconductors are computed in one-space dimension. Such models describe charge transport in semiconductor devices. Two models are taken into consideration. The first one has been developed by Blotekjaer, Baccarani *et al.*, and the second one by Anile *et al.* In both cases the system of equations can be written as a convection-diffusion type system, with a right-hand side describing relaxation effects and interaction with a self-consistent electric field. The numerical scheme is a splitting scheme based on the Nessyahu–Tadmor scheme for the hyperbolic step, and a semi-implicit scheme for the relaxation step. The numerical results are compared to detailed Monte–Carlo simulation.

1. Introduction

Charge transport in semiconductors has recently become an interesting research field in applied mathematics.

The model that has been used in engineering applications is the so-called *drift-diffusion* model.[1,2] Such model, however, is not accurate enough for submicron devices, and several relevant physical effects, such as inertial effects, are not captured by this model.

For devices with channel length of some tenths of micron, when direct quantum effects are negligible, an accurate physical description is given by semiclassical kinetic models. The carriers are described by a density function in phase space,

*E-mail: romano@dipmat.unict.it
†E-mail: russo@univaq.it

satisfying a Boltzmann-like equation. The most effective technique for the numerical solution of such equation is Monte–Carlo simulation. However, computational times required for an accurate solution are too large for a widespread use of Monte–Carlo simulation as a practical CAD tool of semiconductor devices. It is therefore desirable to approximate the transport equation with simpler models which are accurate enough to maintain relevant physical effects of charge transport in submicron devices, and much faster to solve than kinetic models.

The drift-diffusion models can be derived from the kinetic equation by the Chapman–Enskog expansion.[3] These models are commonly used for device simulations. They provide a reasonable approximation when the channel length is large enough (say more than a few microns) with applied voltage of the order of one Volt. The evolution of the carriers is described by a balance equation, where the current is assumed a function of the density and density gradient.

With the reduction of the size of the devices, and the increase in electric field, the drift-diffusion approximation is no longer satisfying, and more sophisticated models are necessary, which are able to describe carrier evolution under the effect of high electric field.

Blotekjaer,[4] Baccarani and Wordeman[5] proposed a model (BBW) which is the analogue of the classical Navier–Stokes–Fourier model for dissipative fluids.

In BBW model, electrons are treated as an inviscid, thermal conducting, monoatomic gas. Heat flux is given by an empirical Fourier law, with a thermal conductivity that contains a fitting parameter. The latter is chosen to fit experimental data or Monte–Carlo simulations. This expression for the heat flux has been recently criticized by Stettler[6] and Tang,[7] who suggest to add an empirical convective term in the heat flux.

Anile *et al.*[8] (which we denote by AP) proposed a model based on *extended thermodynamics*.[9,10] They obtain in a consistent way an expression for the heat flux which contains a convective term, and has no fitting parameter, because all transport coefficients are obtained from the theory.

In this paper we perform a numerical integration of the equations of AP and BBW models. As a test problem we consider the simulation of a n^+–n–n^+ diode in 1-D. The time-dependent problem is solved. The stationary solution is obtained as a limit of the time-dependent solution for large enough time. The numerical solutions are then compared with detailed Monte–Carlo simulations obtained by the DAMOCLES code developed by IBM.[11,12]

The mathematical structure of the system of equations is the same for both models. The differential part of the system can be written as a sum of hyperbolic and parabolic terms. The right-hand side contains a relaxation term, which describes the interaction with the lattice, and a drift term due to the electric field. The latter is self-consistently computed via Poisson's equation.

The numerical scheme used is based on a splitting scheme. In the first step the hyperbolic part is solved, and in the second step diffusion, relaxation, and drift terms are computed. The hyperbolic step is solved by a variant of second-order

shock-capturing TVD scheme, recently developed by Nessyahu and Tadmor.[13] A uniformly non oscillatory reconstruction from cell averages is used.

A similar problem was consider in Ref. 14 by using ENO schemes. The choice of the NT scheme is motivated by the following considerations. First we observe that, because of the convective term in the heat flux for AP model, the hyperbolic part of the equations is different from that of Euler's equations and there is no simple analytical expression of the characteristic speeds. The second reason is that more complex models can be derived by extended thermodynamics.[15] They are described by hyperbolic systems with relaxation, and also in this case there is no simple expression for the characteristic speeds, therefore it is not practical to use upwind-based methods. NT scheme does not require the computation of the eigenvalues of the system, since the building block is Lax–Friedrichs scheme.

The plan of the paper is as follows: In Sec. 2 we briefly recall the kinetic formulation, the drift-diffusion model, and the two hydrodynamical models (BBW and AP). In Sec. 3 we describe the numerical method used in the computation and Sec. 4 is devoted to the numerical results.

2. Mathematical Models for Semiconductors

In a doped semiconductor, the carriers (electrons and holes) move under the influence of the electric field, and interact with phonons and impurities of the crystal.

Energy transport in crystal is mainly carried by phonons.[16] A detailed physical description of transport phenomena requires a three-component model — electrons, phonons and holes, each of which satisfies a quantum transport equation coupled with Maxwell's equations for the electromagnetic field.

Carrier speed is at least three orders of magnitude smaller than light speed, and therefore it is justified to neglect effect of the magnetic field induced by the currents. A quasistatic approximation is assumed, where the self-consistent electric field $\mathbf{E}$ is coupled to the system through the Poisson equation.

Furthermore, we shall neglect generation-recombination effects, whose characteristic time is of the order of nanoseconds. The relaxation of our system, in fact, takes place in times of the order of few picoseconds.

From now on we consider only one family of carriers, namely electrons. We shall assume that phonons are in thermodynamical equilibrium and neglect the effect of the heating of the crystal. Therefore the phonons are described by an equilibrium distribution at temperature T_0.

In a semiclassical kinetic description, the electron dynamics is described by a transport equation for a one-particle distribution function $f(\mathbf{x}, t, \mathbf{k})$, which represents the probability density to find a particle at time t at position $\mathbf{x}$ and with momentum $\mathbf{k}$,

$$\frac{\partial f}{\partial t} + v^i(\mathbf{k})\frac{\partial f}{\partial x^i} - eE^i\frac{\partial f}{\partial k^i} = \mathcal{C}[f]\,. \tag{2.1}$$

Here e represents the (positive) electron charge, $\mathbf{E}$ the electric field, $\mathbf{k}$ the electron impulse, belonging to the first Brillouin zone.[2,a]

$\mathcal{C}[f]$ is the collision term that describes the scattering with acoustical and optical phonons. Electron velocity $v(\mathbf{k})$ depends on the energy of the conduction band via the dispersion relation,

$$v(\mathbf{k}) = \nabla_{\mathbf{k}} \mathcal{E} \,.$$

In general, the band structure may be very complicated and depends on the type and doping of the semiconductor. We shall consider a single band with parabolic approximation. The energy is therefore given by

$$\mathcal{E} = \frac{k^2}{m^*} \,,$$

where m^* is electron effective mass. In this approximation, electron velocity is given by

$$v^i = \frac{k^i}{m^*} \,.$$

Consistently, the first Brillouin zone is extended to $\mathbf{R}^3$.

Equation (2.1) is a nonlinear integrodifferential equation in seven variables and its use as a CAD tool is not practical on account of the numerical difficulties which require too expensive computing time. This has prompted the formulation of macroscopic models.

By introducing electron number density n and flux $\mathbf{F}$ by

$$n = \int d\mathbf{k} f \quad \text{and} \quad \mathbf{F} = \int d\mathbf{k} \frac{\mathbf{k} f}{m^*} \,,$$

and integrating Eq. (2.1) with respect to $\mathbf{k}$ one obtains the balance equation for the density

$$\frac{\partial n}{\partial t} + \frac{\partial F^i}{\partial x^i} = R - G \,, \tag{2.2}$$

where $R - G$ is the electron-hole generation-recombination term (which we shall neglect).

Under the assumption that the electron temperature is equal to the (constant) lattice temperature T_0, and by introducing the mobility

$$\mu_n = \frac{(4\pi)^2 e}{3 m^* k_{\mathrm{B}} T_0 n} \int dk \, f_{\mathrm{eq}} k^4 \tau(\mathcal{E}(\mathbf{k})) \,,$$

one obtains

$$\mathbf{F} = \mu_n n \nabla \phi - D_n \nabla n \,, \tag{2.3}$$

where the diffusion coefficient is given by $D_n = \mu_n k_{\mathrm{B}} T_0 / e$.

[a]Einstein summation over repeated indices is assumed. Physical units are such that $\hbar = 1$.

Equation (2.3), coupled with the analogue equation for holes and with the Poisson equation, constitute the well-known drift-diffusion model.[1,2]

For submicron devices, with electric potential of the order of 1 V, the assumption of constant electron temperature is no longer valid, since the electric field is strong enough to prevent thermodynamical equilibrium. It is therefore necessary to have a more detailed description of transport phenomena. Modified versions of the classical drift-diffusion model have been proposed, which include some effects related to temperature gradients.[17,18] However hydrodynamical models seem more suitable to describe nonequilibrium effects. In BBW model, electrons are treated as an inviscid, thermal conducting fluid. The system is described by continuity equation, momentum balance equation and energy balance equation,

$$\frac{\partial}{\partial t} n + \frac{\partial}{\partial x^i}(n v_i) = 0\,, \tag{2.4}$$

$$\frac{\partial}{\partial t}(n v_i) + \frac{\partial}{\partial x^j}\left(n v_i v_j + \frac{p}{m^*}\delta_{ij}\right) = -\frac{n v_i}{\tau_p} - neE_i\,, \tag{2.5}$$

$$\frac{\partial}{\partial t}\left(\frac{n v^2}{2} + \frac{3}{2}\frac{p}{m^*}\right) + \frac{\partial}{\partial x^i}\left[\left(\frac{n v^2}{2} + \frac{5p}{2m^*}\right) v_i + \frac{q_i}{m^*}\right] = -\frac{W - W_0}{m^* \tau_W} - \frac{n e v_i E^i}{m^*}\,, \tag{2.6}$$

coupled to the Poisson equation

$$\varepsilon \Delta \phi = -e(N_D - N_A - n)\,.$$

Here N_A is the acceptor density, N_D the donor density, ε the dielectric constant, $W_0 = \frac{3}{2} n k_{\mathrm{B}} T_0$. W is the energy density given by

$$W = \frac{1}{2} n m^* v^2 + \frac{3}{2} n k_{\mathrm{B}} T\,,$$

where T is the electron temperature, which is related to the pressure p by ideal gas law

$$p = n k_{\mathrm{B}} T\,.$$

The heat flux satisfies Fourier's law

$$q_i = -kn \frac{\partial T}{\partial x^i}\,,$$

where

$$k = \left(\frac{5}{2} + c\right) k_{\mathrm{B}}^2 \frac{T \tau_p}{m^*}\,.$$

c is a free parameter, whose value is chosen in order to fit experimental data or Monte–Carlo simulations.

Relaxation times are given by the following phenomenological expressions

$$\tau_p = \frac{m^* \mu_n T_0}{eT}\,,$$

$$\tau_W = \mu_n T_0 \left(\frac{m^*}{2eT} + \frac{3k_{\mathrm{B}}T}{2ev_S^2(T+T_0)} \right),$$

where μ_n is low field mobility and v_S is the saturation velocity.

BBW equations have been solved numerically in both the stationary[19,20] and nonstationary cases.[14]

This model, however, does not have the correct limit near thermodynamical equilibrium,[21] since it does not satisfy Onsager's reciprocity conditions.[22] Moreover, the constitutive assumption on the heat flux has no theoretical justification.

A recent formulation of constitutive equations, in better agreement with the linear theory of irreversible process, has been obtained for the heat flux by Anile *et al.*[8] The formulation is based on the theory of extended thermodynamics[9,10] (the same derivation can be obtained by the moment method approach of Levermore[23]).

The model is constituted, as for the BBW one, by the balance equations of electron density, momemtum and energy

$$\frac{\partial}{\partial t} n + \frac{\partial}{\partial x^i}(nv_i) = 0\,, \tag{2.7}$$

$$\frac{\partial}{\partial t}(nv_i) + \frac{\partial}{\partial x^j} F_{ij} = Q_i - neE_i\,, \tag{2.8}$$

$$\frac{\partial}{\partial t}\left(\frac{nv^2}{2} + \frac{3}{2}\frac{p}{m^*} \right) + \frac{\partial}{\partial x^i} S_i = -\frac{W - W_0}{m^* \tau_W} - \frac{nev_i E^i}{m^*}\,, \tag{2.9}$$

where, according to the kinetic theory of gases,

$$F_{ij} = \int \frac{d\mathbf{k} f k_i k_j}{(m^*)^2}$$

is the flux momentum density and

$$S_i = \frac{1}{2} \int \frac{d\mathbf{k} f k_i k^2}{(m^*)^3}$$

is flux energy density.

By employing the methods of extended thermodynamics, followed by the so-called *Maxwellian iteration*[8,21,24] (a procedure similar to the Chapman–Enskog expansion of the Boltzmann equation), the following relations have been obtained[8]

$$F_{ij} = nv_i v_j + \frac{p}{m^*}\delta_{ij}\,,$$

$$S_i = \frac{1}{2} nv^2 v_i + \frac{1}{m^*}\left(\frac{5}{2} p v_i + q_i \right),$$

with the following constitutive equation for the heat flux q_i

$$q_i = -\frac{5nk_{\mathrm{B}}^2 T\tau_q}{2m^*}\frac{\partial T}{\partial x^i} + \frac{5}{2}\, nk_{\mathrm{B}} T v_i \left(\frac{1}{\tau_p} - \frac{1}{\tau_q}\right)\tau_q\,, \tag{2.10}$$

τ_q being the energy flux relaxation time.

At variance with BBW model, Eq. (2.10) does not contain free parameters. Moreover, due to the presence of the convective term in the constitutive equation for the heat flux, Onsager relations for small deviations from thermodynamical equilibrium are satisfied.[21]

About production terms, we shall use the same approximation used in BBW, but with relaxation times given by Monte–Carlo simulation.

3. Numerical Method

Let us write the 1-D version of the equations of the two models:

$$\frac{\partial}{\partial t} n + \frac{\partial}{\partial x}(nv) = 0\,, \tag{3.11}$$

$$\frac{\partial}{\partial t}(nv) + \frac{\partial}{\partial x}\left(nv^2 + \frac{p}{m^*}\right) = -\frac{nv}{\tau_p} - neE\,, \tag{3.12}$$

$$\frac{\partial}{\partial t}\left(nv^2 + 3\frac{p}{m^*}\right) + \frac{\partial}{\partial x}\left(nv^3 + \frac{5pv}{m^*} + \frac{2q}{m^*}\right) = -2\frac{W - W_0}{m^*\tau_W} - \frac{2nevE}{m^*}\,. \tag{3.13}$$

Heat flux q is given by

$$q = -\frac{5nk_{\mathrm{B}}^2 T\tau_q}{2m^*}\frac{\partial T}{\partial x} + \frac{5}{2} nk_{\mathrm{B}} T v \left(\frac{\tau_q}{\tau_p} - 1\right) \tag{3.14}$$

for AP model and by

$$q = -\left(\frac{5}{2} + c\right) nk_{\mathrm{B}}^2 \frac{T\tau_p}{m^*}\frac{\partial T}{\partial x}$$

for BBW model. The equations must be supplemented with Poisson's equation.

For future reference it is better to write the previous equations in a more compact form. Let us define the following vector fields:

$$\mathbf{u} = (n, nv, 2W)\,,$$

$$\mathbf{f}_{\mathrm{BBW}} = \left(nv, nv^2 + \frac{p}{m^*}, nv^3 + \frac{5pv}{m^*}\right),$$

$$\mathbf{f}_{\mathrm{AP}} = \left(nv, nv^2 + 3\frac{p}{m^*}, nv^3 + 5\frac{pv}{m^*}\frac{\tau_q}{\tau_p}\right),$$

$$\mathbf{g}_{\mathrm{BBW}} = \left(0, -\frac{nv}{\tau_p} - \frac{nE}{m^*}, -2\frac{W - W_0}{m^*\tau_w} - \frac{2nvE}{m^*} + \frac{2}{m^*}\frac{\partial}{\partial x}\left(kn\frac{\partial T}{\partial x}\right)\right),$$

$$\mathbf{g}_{\mathrm{AP}} = \left(0, -\frac{nv}{\tau_p} - \frac{nE}{m^*}, -2\frac{W - W_0}{m^*\tau_w} - \frac{2nvE}{m^*} + \frac{1}{m^*}\frac{\partial}{\partial x}\left(\frac{5nk_{\mathrm{B}}^2 T\tau_q}{m^*}\frac{\partial T}{\partial x}\right)\right).$$

The systems are then written as

$$\frac{\partial \mathbf{u}}{\partial t} + \frac{\partial \mathbf{f}_{\mathrm{BBW}}}{\partial x} = \mathbf{g}_{\mathrm{BBW}} \tag{3.15}$$

for BBW model and

$$\frac{\partial \mathbf{u}}{\partial t} + \frac{\partial \mathbf{f}_{\mathrm{AP}}}{\partial x} = \mathbf{g}_{\mathrm{AP}} \tag{3.16}$$

for AP model.

The left-hand side of Eqs. (3.15) and (3.16) represents a quasilinear hyperbolic operator, while the right-hand side contains relaxation, diffusion and drift terms. We make use of a splitting scheme, based on the following decomposition. Let us consider a system of the form

$$\frac{\partial \mathbf{u}}{\partial t} + \frac{\partial \mathbf{f}}{\partial x} = \mathbf{g}\,. \tag{3.17}$$

Then, for each time step, a numerical approximation $\tilde{\mathbf{u}}$ of the solution is obtained by solving the two consecutive steps:

$$\left.\begin{aligned} &\frac{\partial \mathbf{u}_1}{\partial t} + \frac{\partial \mathbf{f}}{\partial x} = 0 \\ &\mathbf{u}_1(t) = \tilde{\mathbf{u}}(t) \end{aligned}\right\} \quad \text{convection step} \tag{3.18}$$

$$\left.\begin{aligned} &\frac{\partial \tilde{\mathbf{u}}}{\partial t} = \mathbf{g} \\ &\tilde{\mathbf{u}}(t) = \mathbf{u}_1(t + \Delta t)\,. \end{aligned}\right\} \quad \text{relaxation step} \tag{3.19}$$

We shall call this scheme *simple splitting* (SP). Note that this scheme is only first order in time, independently of the accuracy of the solution of the two steps.

A better scheme is obtained by a more sophisticated splitting strategy, as shown in Sec. 3.3.

3.1. *Convection step*

During the convection step one integrates the quasilinear hyperbolic system (3.18). It is well known that the solutions of such systems suffer loss of regularity and may develop discontinuities. There is a wide literature on shock capturing schemes for hyperbolic systems of conservation laws, which are second-order accurate in space in the region of regularity, and give sharp shock profile. A recent account on numerical methods for conservation laws was given in Ref. 25. Higher order methods have been developed and used for solving problems in semiconductor device simulation, such as ENO schemes (see Ref. 14). Such schemes, however, require an exact or approximate Riemann solver, or at least the knowledge of the characteristic structure of the Jacobian matrix. For systems similar to gas dynamics, an approximate Riemann solver based on the Roe matrix is used. Such approach is suitable in the case of BBW model, since the hyperbolic operator is the same as the one in gas dynamics, and

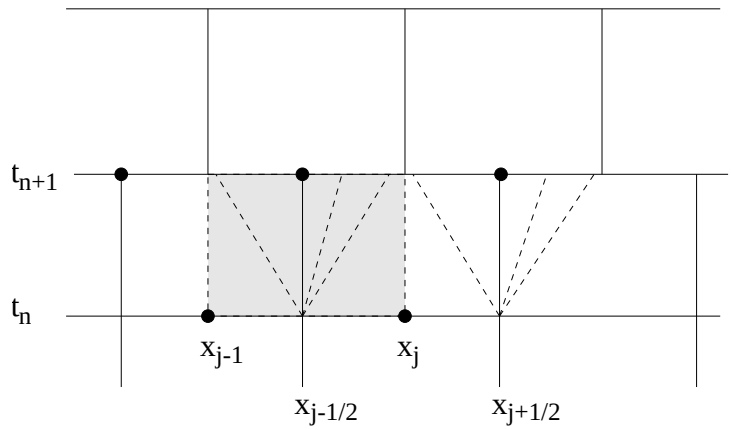

Fig. 1. NT scheme on a staggered grid.

therefore the analytical expression for the eigenvalues and eigenvectors is explicitly known. In AP model, the presence of the term τ_q/τ_p does not allow us to write down a simple analytical expression for the eigenvalues of the system (see Sec. 3.2). Therefore it is desirable to use a shock-capturing scheme that does not require the explicit knowledge of the characteristic structure of the system. The scheme proposed by Nessyahu and Tadmor (NT)[13] has these properties. Its building block is Lax–Friedrichs scheme, corrected by a MUSCL type interpolation that guarantees second-order in smooth regions and TVD property.[26]

For the sake of completeness, we report the derivation of NT scheme and UNO reconstrution. For more details, see Refs. 13 and 27.

Let us consider a system of the form

$$\frac{\partial v}{\partial t} + \frac{\partial f(v)}{\partial x} = 0\,, \tag{3.20}$$

where $v \in \mathbf{R}^m$ and $f : \mathbf{R}^m \to \mathbf{R}^m$. We introduce a uniform grid in $x, x_1, x_2, \ldots, x_N$, and in $t, t_1, t_2, \ldots$.

By integrating Eq. (3.20) on a cell $[x_j, x_{j+1}] \times [t_n, t_{n+1}]$, one obtains

$$\overline{v}_{j+1/2}(t_n + \Delta t) = \overline{v}_{j+1/2}(t_n) - \frac{1}{\Delta x}\left[\int_{t_n}^{t_n+\Delta t} f(v(x_{j+1},\tau))\,d\tau - \int_{t_n}^{t_n+\Delta t} f(v(x_j,\tau))\,d\tau\right], \tag{3.21}$$

where

$$\overline{v}_{j+1/2}(t_n) = \frac{1}{\Delta x}\int_{x_j}^{x_{j+1}} v(y,t_n)\,dy$$

represents the cell average of $v(x,t)$ in $[x_j, x_{j+1}]$ for $t = t_n$. The integral of the flux $f(v(x,t))$ is computed by the midpoint quadrature rule:

$$\int_{t_n}^{t_n+\Delta t} f(v(x_j,\tau))\,d\tau = \Delta t f\left(v(x_j, t_n + \frac{\Delta t}{2}\right) + O(\Delta t^3)\,. \tag{3.22}$$

The quantity $v(x_j, t_n+\Delta t/2)$, is computed according to Lax–Wendroff approach, by using Taylor's formula:

$$v\left(x_j, t + \frac{\Delta t}{2}\right) = v_j(t) - \frac{1}{2}\lambda f'_j + O(\Delta t^2)\,, \tag{3.23}$$

where $f'_j/\Delta x$ is an approximation of the space derivative of the flux (yet to be specified) and $\lambda = \Delta t/\Delta x$. In order to obtain a second-order scheme we require that

$$\frac{1}{\Delta x} f'_j = \frac{\partial}{\partial x} f(v(x,t)) + O(\Delta x)\,.$$

By substituting (3.22) into (3.21), one has a relation that involves both cell averages and point values of the solution.

By introducing a MUSCL interpolation, we approximate $v(x,t)$ by a piecewise linear polynomial

$$L_j(x,t) = v_j(t) + (x - x_j)\frac{1}{\Delta x}\, v'_j\,, \quad x_{j-1/2} \le x \le x_{j+1/2} \tag{3.24}$$

and in order to ensure a second-order accuracy we require that

$$\frac{1}{\Delta x}\, v'_j = \frac{\partial}{\partial x}\, v(x_j,t) + O(\Delta x)\,. \tag{3.25}$$

Therefore, Eq. (3.21), together with (3.22)–(3.24), gives

$$\begin{aligned}\overline{v}_{j+1/2}(t+\Delta t) = {} & \frac{1}{2}\left[v_j(t) + v_{j+1}(t)\right] + \frac{1}{8}\left[v'_j - v'_{j+1}\right] \\ & - \lambda\left[f\left(v_{j+1}(t_n) - \frac{1}{2}\,\lambda f'_{j+1}\right) - f\left(v_j(t_n) - \frac{1}{2}\,\lambda f'_j\right)\right] + O(\Delta t^3)\,.\end{aligned}$$

Since the initial state at $t = t_n$ is given by the piecewise linear function $L_j(x,t_n)$, the fluxes remain regular functions if the solutions of the corresponding generalized Riemann problems between adjacent cells do not interact.

This is obtained by imposing the following CFL condition

$$\lambda \cdot \rho(A(v(x,t))) < \frac{1}{2}\,, \tag{3.26}$$

where $\rho(A(v(x,t)))$ is the spectral radius of the Jacobian matrix,

$$A = \frac{\partial f}{\partial v}\,.$$

In this way a family of predictor–corrector schemes is obtained:

$$v_j^{n+1/2} = v_j^n - \frac{1}{2}\,\lambda f_j'\,,$$

$$v_{j+1/2}^{n+1} = \frac{1}{2}\,[v_j^n + v_{j+1}^n] - \lambda[g_{j+1} - g_j]\,,$$

where

$$g_j = f(v_j^{n+1/2}) + \frac{1}{8\lambda} v_j'\,.$$

Such schemes are conservative and consistent, which is a necessary requirement for correct shock capturing.

In order to determine the expression of v_j' and f_j', we make use of a uniform non oscillatory reconstruction,[27] which guarantees uniform second-order accuracy (even near local extrema) for smooth solutions.

Starting from cell average of $v(x,t)$, one constructs a piecewise quadratic polynomial $Q(x,t)$, such that

$$Q(x_j,t) = v(x_j,t) + O(\Delta x^3)\,,$$

$$\frac{d}{dx}\,Q(x \pm 0,t) = \frac{dv(x,t)}{dx} + O(\Delta x^2)\,,$$

when $v(x,t)$ is a regular function.

The required condition on $Q(x,t)$ is to be nonoscillatory, in the sense that its number of local extrema is not larger than that of $v(x,t)$. This is obtained with an appropriate choice of the stencil.

For $x_j \le x \le x_{j+1}$, the two candidates to $Q(x,t)$ are the polynomial interpolating the function on the nodes x_{j-1}, x_j, x_{j+1}, and the one interpolating the function on the nodes x_j, x_{j+1}, x_{j+2}. The one which is closer to the line through points $(x_j, v(x_j,t))$ and $(x_{j+1}, v(x_{j+1},t))$ is chosen.

In the interval $x_j \le x \le x_{j+1}$ we write

$$Q(x,\cdot) = v_j + d_{j+1/2}\,v\frac{x - x_j}{\Delta x} + \frac{1}{2}\,D_{j+1/2}\,v\frac{(x - x_j)(x - x_{j+1})}{(\Delta x)^2}\,,$$

with

$$d_{j+1/2}\,v = v_{j+1} - v_j\,.$$

Then one has

$$D_{j+1/2}\,v = v_{j+1} - 2v_j + v_{j-1}$$

if we choose x_{j-1}, x_j, x_{j+1} and

$$D_{j+1/2}\,v = v_{j+2} - 2v_{j+1} + v_j$$

if we choose x_j, x_{j+1}, x_{j+2}.

This choice can be expressed in the form

$$D_{j+1/2}\,v = \mathrm{MM}(v_{j+2} - 2v_{j+1} + v_j, v_{j+1} - 2v_j + v_{j-1})\,, \tag{3.27}$$

where $\mathrm{MM}(x,y)$ is the min mod function, defined by

$$\mathrm{MM}(x,y) = \begin{cases} \mathrm{sgn}(x)\cdot\min(|x|,|y|) & \text{if } \mathrm{sgn}(x)=\mathrm{sgn}(y) \\ 0 & \text{otherwise}\,. \end{cases}$$

We can compute the slope of $L_j(x,t)$ by

$$\frac{v'_j}{\Delta x} = \mathrm{MM}\left(\frac{d}{dx}\,Q(x_j-0,t), \frac{d}{dx}\,Q(x_j+0,t)\right),$$

that is by

$$v'_j = \mathrm{MM}\left(d_{j-1/2}\,v + \frac{1}{2}\,\mathrm{MM}(D_{j-1},D_j), d_{j+1/2}\,v - \frac{1}{2}\,\mathrm{MM}(D_j,D_{j+1})\right), \quad (3.28)$$

where

$$D_j = v_{j+1} - 2v_j + v_{j-1}\,.$$

The computation of f'_j can be obtained by a similar reconstruction, from the values of $f(\overline{v}^n_j)$, or by the Jacobian matrix

$$f'_j = \frac{\partial f}{\partial v}\,(v_j)v'_j\,.$$

Due to the staggered grid, we perform the convection step by two NT steps, so that the field for the relaxation step is computed on a non-staggered grid.

3.2. *Relaxation step*

The relaxation step has been solved by a semi-implicit Euler scheme, in order to avoid stability restriction on the time step Δt. In the case of AP model the equations are

$$\frac{\partial n}{\partial t} = 0\,, \quad (3.29)$$

$$\frac{\partial m}{\partial t} = -\frac{m}{\tau_p} - \frac{neE}{m^*}\,, \quad (3.30)$$

$$\frac{\partial 2W}{\partial t} = -2\frac{W-W_0}{\tau_W} - 2meE - 2\frac{\partial q}{\partial x}\,, \quad (3.31)$$

with $m = nv$. During the relaxation step from t_n to t_{n+1} we approximate the relaxation times, τ_p, τ_W and τ_q, to the value that they assume at time t_n.

From Eq. (3.29) we have

$$n_j^{n+1} = n_j^n\,, \quad (3.32)$$

therefore during the relaxation step the electric field E is constant. The electric potential is obtained by solving the tridiagonal system

$$\varepsilon(\phi_{j+1} - 2\phi_j + \phi_{j-1}) = -e(\Delta x)^2(N_D - N_A - n_j^n)$$

by standard procedure.

The electric field is computed from the potential by centered differences.

From Eq. (3.30) one has

$$m_j^{n+1} = \left(m_j^n + \frac{n_j e E_j^n \tau_{pj}^n}{m^*} \right) \exp\left(-\frac{\Delta t}{\tau_{pj}^n} \right) - \frac{n_j^n e E_j^n}{m^*} \tau_{pj}^n \,.$$

It is more convenient to integrate an equation for the temperature T, rather than Eq. (3.31),

$$\frac{\partial T}{\partial t} = \frac{1}{3} \frac{m^*}{k_\mathrm{B}} \left(\frac{2}{\tau_p} - \frac{1}{\tau_W} \right) v^2 - \frac{T - T_0}{\tau_W} + \frac{5 k_\mathrm{B}}{3 n m^*} \frac{\partial}{\partial x} \left[n \tau_q T \frac{\partial T}{\partial x} \right] . \tag{3.33}$$

Let

$$A = \frac{5 k_\mathrm{B}}{3 n m^*} \,,$$

$$H = \frac{1}{3} \frac{m^*}{k_\mathrm{B}} \left(\frac{2}{\tau_p} - \frac{1}{\tau_W} \right) v^2 + \frac{T_0}{\tau_W} \,,$$

$$G = n \tau_q \,.$$

Then Eq. (3.33) is discretized as

$$\frac{T_j^{n+1} - T_j^n}{\Delta t} = - \frac{T_j^{n+1}}{\tau_{W\,j}} + \frac{A_j}{(\Delta x)^2} \left[(GT)_{j+1/2}^n (T_{j+1}^{n+1} - T_j^{n+1}) \right.$$

$$\left. - (GT)_{j-1/2}^n (T_j^{n+1} - T_{j-1}^{n+1}) \right] + H_j \,,$$

where, for any quantity h defined on the grid, we denote

$$h_{j+1/2} \equiv \frac{h_{j+1} + h_j}{2} \,.$$

Once again we obtain a tridiagonal system for T_j^{n+1} which can be solved by standard technique.

A similar procedure has been used in order to integrate the BBW equations.

Note that the relaxation step is second-order accurate in space, but only first order accurate in time. However, it can be used to construct second-order schemes, as described in Sec. 3.3.

3.3. *Second-order splitting*

Because of the splitting, scheme SP is not second-order accurate even for the computation of steady state solutions.

Accuracy can be improved by using a better splitting strategy.

A second-order scheme, uniformly accurate in the relaxation times, has been developed in Ref. 28 for a second-order upwind convection step. Different splitting methods, that use the NT convection step, have been considered in Ref. 29.

A suitable generalization to the case where an electric field is present, is given by the following steps: Given the fields at time t_n, (U^n, E^n), the fields at time t_{n+1}

are obtained as

$$
\begin{aligned}
U_1 &= U^n - R(U_1, E^n, \Delta t)\,,\\
U_2 &= \frac{3}{2}U^n - \frac{1}{2}U_1\,,\\
U_3 &= U_2 - R(U_3, E^n, \Delta t)\,,\\
U_4 &= \mathcal{C}_{\Delta t} U_3\,,\\
E^{n+1} &= \mathcal{P}(U_4)\,,\\
U^{n+1} &= U_4 - R(U^{n+1}, E^{n+1}, \Delta t/2)\,,
\end{aligned}
$$

where R represents the numerical operator corresponding to relaxation step, $\mathcal{C}_{\Delta t}$ represents the numerical convection operator corresponding to two steps of NT scheme, $\mathcal{P}(U)$ gives the solution of Poisson's equation.

4. Numerical Results

As test problem we consider the numerical solution of a ballistic diode n^+–n–n^+, which models the channel of a MOSFET. The device is made of silicon and its temperature is 300 K. The n^+ regions are 0.1 μm long, and the n region is 0.4 μm long. In n^+ regions the doping density is $n_0 = 10^{18}$ cm^{-3}, and in the n region the doping density is $n_0 = 10^{16}$ cm^{-3}.

The effective electron mass, in the approximation of parabolic band, is $m^* = 0.32\ m_e$ where m_e is the electron mass.[30] The dielectric constant of silicon is $\varepsilon = \varepsilon_r \varepsilon_0$, where $\varepsilon_r = 11.7$ is the relative dielectric constant and $\varepsilon_0 = 8.85 \times 10^{-18}$ C/Vμm is the dielectric constant of vacuum. The saturation velocity is $v_S = 1.03 \times 10^{17}$ cm/sec.

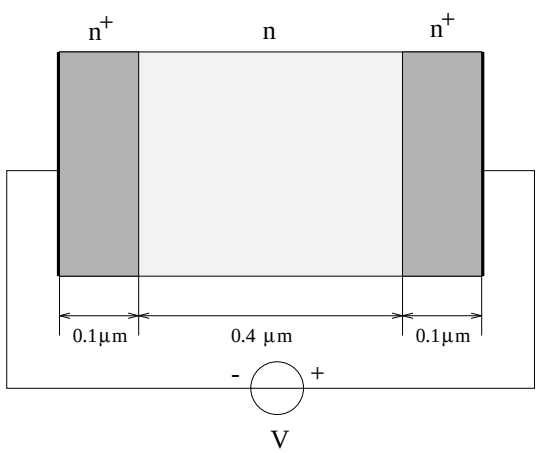

Fig. 2. n^+–n–n^+ diode.

Relaxation times τ_W, $\tau_p\,\tau_q$, respectively of energy, momentum and energy flux, have been obtained by a fitting of the results of Monte–Carlo simulations.[12] They can be expressed as function of the total energy per electron, by the following formulas

$$\tau_A = a + b(\mathcal{E} - 1) + c\exp(-d(\mathcal{E} - 1))\,,$$

where $\tau_A = \tau_p, \tau_W, \tau_q$, with

$$\mathcal{E} = \frac{\text{energy per electron in eV}}{0.025\ \text{eV}}\,.$$

Coefficients a, b, c and d are reported in Tables 1 and 2.

Table 1. Coefficients for the fitting of relaxation times.

	τ_p	τ_W	τ_q
a	0.0681	0.1731	0.0471
b	−0.0023	0.0313	−0.0007
c	0.2051	0.2382	0.1330
d	0.9547	0.5167	0.6911

Table 2. Numerical convergence study for the simple splitting scheme. Stationary solution AP model. L^1 and L^∞ norms of relative errors.

		200–400 points	400–800 points	convergence rate
L^1	velocity	0.0044	0.0018	1.275
Norm	energy	0.0027	0.0010	1.392
L^∞	velocity	0.0433	0.0140	1.631
Norm	energy	0.0199	0.0059	1.751

In Fig. 3 we give the values of the relaxation times that have been used in the calculations, for a channel length of 0.4 μm. It appears that $\tau_q/\tau_p \neq 1$, and therefore it is not justified to neglect the convective term in the expression for the heat flux.

Initially the temperature is uniform at 300 K, and the charges do not move. Then an external voltage of 1 V is applied, that causes a flux of charges in the semiconductor.

The following initial conditions are assumed

$$n(x,0) = n_0(x)\,, \quad T(x,0) = 300\ \text{K}\,, \quad v(x,0) = 0\,, \quad q(x,0) = 0\,. \qquad (4.34)$$

The initial values for n_0 have been obtained by smoothing the discontinuities in the doping profile by a hyperbolic tangent:

$$n_0(x) = n_0 - d_0\left(\tanh\frac{x - x_1}{s} - \tanh\frac{x - x_2}{s}\right).$$

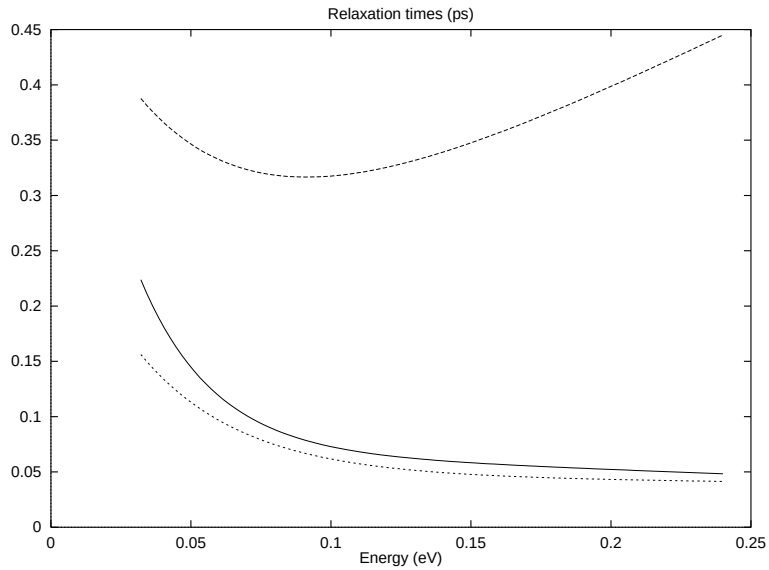

Fig. 3. Relaxation times fitted from Monte–Carlo calculations: τ_W (dashed line), τ_p (continuous line) and τ_q (dotted line).

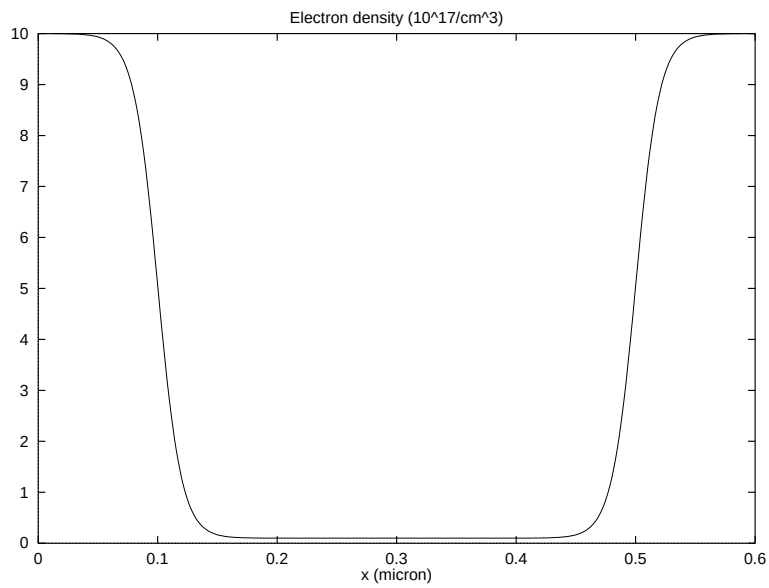

Fig. 4. Doping profile.

We have: $n_0 = n_0(0)$, $d_0 = n_0(1 - 10^{-2})/2$, $s = 0.02$ μm, $x_1 = 0.1$ μm and $x_2 = 0.5$ μm (see Fig. 4).

We now discuss the boundary conditions. The number of independent boundary conditions for a hyperbolic system on each boundary should be equal to the number

of characteristics entering the domain on that portion of the boundary. The other boundary conditions should be given consistent to the field equations. Following Ref. 14, we set

$$n(0,t) = n(L,t) = 10^{18}\ \mathrm{cm}^{-3}\,, \tag{4.35}$$

$$\frac{\partial}{\partial x}\,T(0,t) = \frac{\partial}{\partial x}\,T(L,t) = 0\,, \tag{4.36}$$

$$\frac{\partial}{\partial x}\,v(0,t) = \frac{\partial}{\partial x}\,v(L,t) = 0\,, \tag{4.37}$$

$$e\phi(0) = T\ln\left(\frac{n(0)}{n_i}\right), \quad e\phi(L) = T\ln\left(\frac{n(L)}{n_i}\right) + eV_b\,, \tag{4.38}$$

where n_i =1.4×10^{10} cm^{-3} is the intrinsic electron concentration and V_b is the applied bias voltage. The assignement of a redundant number of boundary conditions is justified by the fact that in the n^+ regions the profiles of the field variables are quite flat. The compatibility with the equations is observed *a posteriori* by the lack of spurious oscillations or reflected waves on the boundary.

Since an implicit scheme has been used in the relaxation step, the only stability limitation is given by the CFL condition on the convection step.

In all the simulations, condition $\Delta t = \Delta x/2c_s$, $c_s \equiv \sqrt{k_{\mathrm{B}}T_0/m^*}$ has been used. Note that the largest eigenvalue of the hyperbolic matrix is always less than c_s and therefore condition (3.26) is always satisfied.

The accuracy study is performed by comparing computations with 200, 400 and 800 grid points. The results for simple splitting are reported in Table 2. 200 grid points give a solution with an L^∞ relative error in velocity less than 5%. Convergence results for the second-order splitting are presented in Table 3. As expected, the latter scheme works better than simple splitting, confirming almost second-order accuracy.

In the expression of the heat flux in BBW model, the values $c = -1$[14,20] and $c = -2.1$[14,31] have been used. The latter provides a better agreement with Monte–Carlo. We remark, however, that those values are not deduced by thermodynamical principles, but are treated as fitting parameters, which may be different for a different device.

Table 3. Numerical convergence study for the second-order splitting scheme. Stationary solution AP model. L^1 and L^∞ norms of relative errors.

		200–400 points	400–800 points	convergence rate
L^1	velocity	0.0040	0.0011	1.814
Norm	energy	0.0016	0.0005	1.506
L^∞	velocity	0.0224	0.0056	1.993
Norm	energy	0.0112	0.0023	2.265

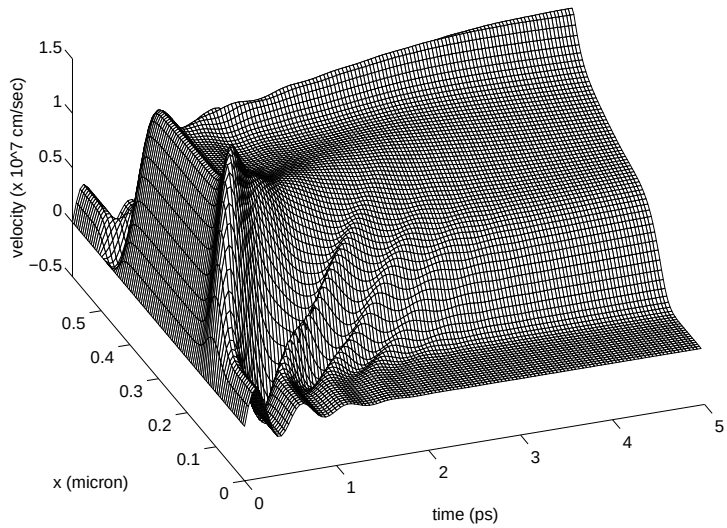

Fig. 5. Time evolution of electron velocity for AP model. Second-order scheme with 200 points.

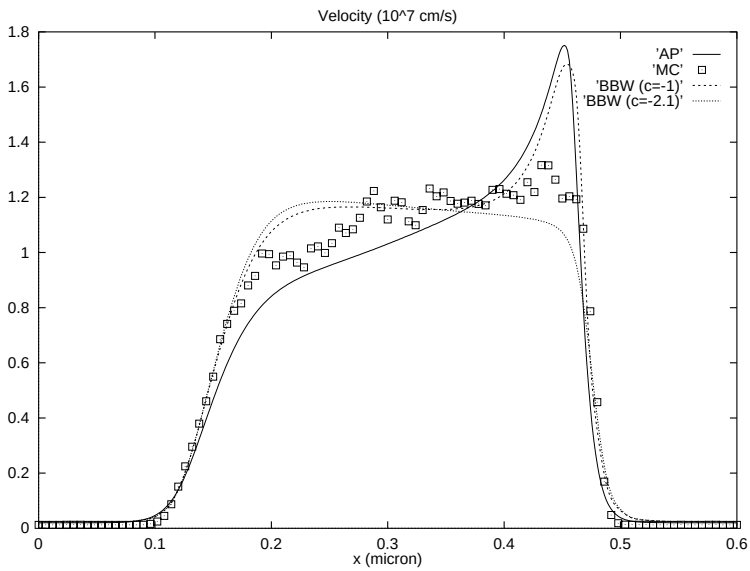

Fig. 6. Velocity profile ($\times 10^7$ cm/sec). AP model (continuous line), BBW model with $c = -1.0$ (dashed line), $c = -2.1$ (dotted line) and with Monte–Carlo DAMOCLES code (squares). The channel length is 0.4 μm, and the applied voltage is 1 V.

In all our simulations, about five picoseconds are enough to reach steady state. In Fig. 5 we report the time evolution of the velocity field. After a rapid transient, steady state regime is approached.

In Figs. 6 and 7 we compare velocity and energy profiles for Monte–Carlo results obtained by the code DAMOCLES,[11] and AP and BBW models for $c = -1$ and

$c = -2.1$, for a channel of length 0.4 μm. If $c = -1$, the two models have roughly the same agreement with Monte–Carlo, while for $c = -2.1$, BBW model shows a better agreement. For both models, the results on energy are more accurate than those on electron velocity. The region with the poorest agreement is near the second junction, because of the peak in the velocity profiles for AP model and for BBW model with $c = -1$.

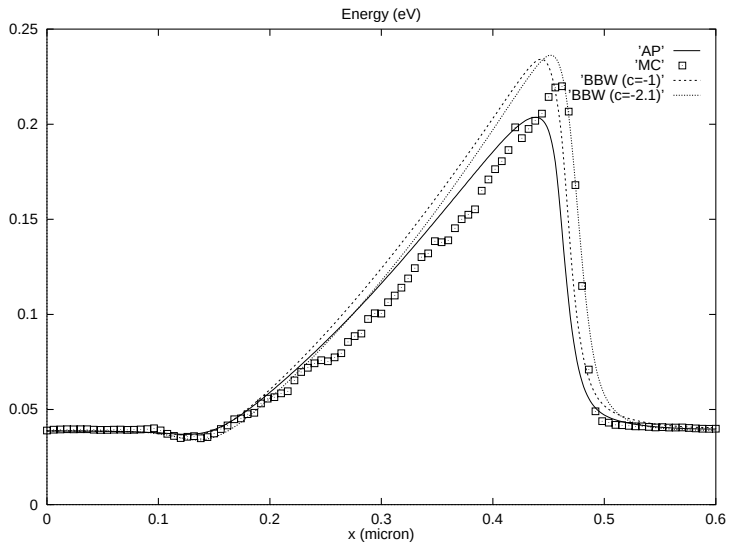

Fig. 7. Energy profile (eV). The notation is as in Fig. 6.

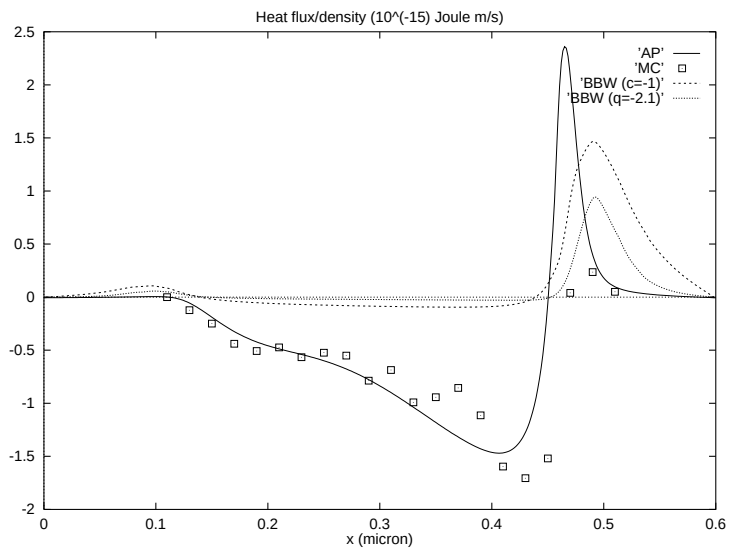

Fig. 8. Heat flux/density (J m/sec). The notation is as in Fig. 6.

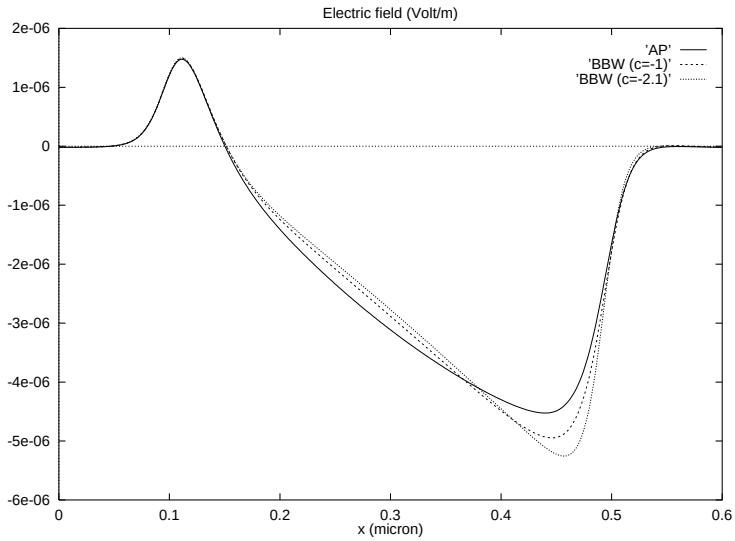

Fig. 9. Electric field (Volt/m). The notation is as in Fig. 6.

The two models show a very different behavior when we consider the heat flux. In the AP model, the convective term constitutes the dominant part (see Fig. 8), and shows a good agreement with Monte–Carlo calculations, except near the second junction. BBW model overestimates the heat flux for both values of c, and the location of the maximum is different. This result is in accordance with what has been observed in Ref. 6, where it was suggested to introduce a convective term in the heat flux, in order to improve the agreement between Monte–Carlo and BBW models.

5. Conclusions

Stationary and non-stationary numerical solutions of recent hydrodynamical models for semiconductors were presented. A numerical scheme has been suitably developed for the purpose. At variance with ENO schemes already used in Ref. 14, our scheme is only second-order in space, but accuracy is maintained in time by a suitable splitting technique. The scheme is quite simple to implement, and it requires neither exact nor approximate Riemann solvers nor the eigenvalues and eigenvectors of the Jacobian matrix of the hyperbolic part of the system. Such property is desirable, since for one of the models there is no simple expression of the characteristic fields.

Two models have been considered: BBW and AP.

A comparison between numerical results and Monte–Carlo simulations shows that BBW model gives satisfactory results for electron velocity and energy, provided a suitable value is chosen for a fitting parameter contained in the expression for the heat conductivity. A bad agreement is observed with Monte–Carlo about the heat flux.

AP model, on the contrary, is derived in a systematic way from a kinetic formulation, by using techniques proper of extended thermodynamics. The model gives a reasonable agreement with Monte–Carlo for the heat flux, but the agreement of velocity and energy profiles is similar to that obtained by BBW model with $c = -1$.

Therefore, although AP model gives a better description of the heat flux, it is not yet satisfactory. We believe that the theoretical foundation of the AP model is physically sound, but the modelling of the production terms needs to be improved. A possible way is to derive the constitutive functions by employing Levermore's theory[23] or the maximum entropy principle[9] which allow one to get closure relations also for the production terms. This could avoid to resort to a fitting of the relaxation times and to lead to a model without free parameters, valid for a general class of electron devices.

Acknowledgments

The authors would like to thank Prof. A. M. Anile for helpful discussion and Dr. O. Muscato who provided the results of the Monte–Carlo simulations obtained by DAMOCLES.

This work has been partially supported by MURST, by CNR project *Modelli matematici per semiconduttori. Progetto speciale: metodi matematici in fluidodinamica e dinamica molecolare*, grant # 96.03855.CT01, and by TMR program *Asymptotic methods in kinetic theory*, grant # ERBFMRXCT970157.

References

1. W. Haensch, **The Drift-Diffusion Equation and Its Application in MOSFET Modeling** (Springer-Verlag, 1991).
2. P. A. Markowich, C. A. Ringhofer and C. Schmeiser, **Semiconductor Equations** (Springer-Verlag, 1990).
3. S. Chapman and T. G. Cowling, **The Mathematical Theory of Nonuniform Gases** (Cambridge Univ. Press, 1970), 3rd ed.
4. K. Blotekjaer, *Transport equation for electrons in two-valley semiconductors*, *IEEE Trans. Electron Devices* **ED-17** (1970) 38–47.
5. G. Baccarani and M. R. Wordeman, *An investigation on steady-state velocity overshoot in Silicon*, *Solid-State Electronics* **29** (1982) 970–977.
6. M. A. Stettler, M. A. Alam and M. S. Lundstrom, *A critical examination of the assumption underlying macroscopic transport equation for silicon device*, *IEEE Trans. Electron Devices* **40** (1993) 733–739.
7. S.-C. Lee and T.-W. Tang, *Transport coefficients for a silicon hydrodynamical model extract from inhomogeneous Monte–Carlo simulation solid-state electronics* **35** (1992) 561–569.
8. A. M. Anile and S. Pennisi, *Thermodynamic derivation of the hydrodynamical model for charge transport in semiconductors*, *Phys. Rev.* **B46** (1992) 13186–13193.
9. I. Müller and T. Ruggeri, **Extended Thermodynamics** (Springer-Verlag, 1993).
10. D. Jou, J. Casas-Vazquez and G. Lebon, **Extended Irreversible Thermodynamics** (Springer-Verlag, 1993).

11. M. V. Fischetti and S. Laux, Phys. *Monte Carlo study of electron transport in silicon inversion layers*, *Phys. Rev.* **B48** (1993) 2244–2274.
12. O. Muscato, R. M. Pidatella and M. V. Fischetti, *Monte Carlo and hydrodynamics simulation of a one dimensional n^+–n–n^+ silicon diode*, *Electronics VLSI Design* **6** (1998) 247–250.
13. H. Nessyahu and E. Tadmor, *Non-oscillatory central differencing for hyperbolic conservation law*, *J. Comput. Phys.* **87** (1990) 408–463.
14. E. Fatemi, J. Jerome and S. Osher, *Solution of hydrodynamic device model using high-order nonoscillatory shock capturing algorithms*, *IEEE Trans. Computer-Aided Design* **10** (1991) 232–398.
15. A. Anile, V. Romano and G. Russo, *Extended hydrodynamical model of carrier transport in semiconductors*, *SIAM J. Appl. Math.*, to appear.
16. N. C. Ashcroft and N. D. Mermin, **Solid State Physics** (Holt-Sounders, 1976).
17. N. Ben Abdallah, P. Degond and S. Genieys, *An energy-transport model for semiconductors derived from the Boltzmann equation*, *J. Stat. Phys.* **84** (1996) 205–231.
18. N. Ben Abdallah and P. Degond, *On a hierarchy of macroscopic models for semiconductors*, *J. Math. Phys.* **37** (1996) 3306–3333.
19. C. L. Gardner, J. W. Jerome and D. J. Rose, *Numerical methods for the hydrodynamic device model: subsonic flow*, *IEEE Trans. Computer-Aided Design* **8** (1989) 501–507.
20. C. L. Gardner, *Numerical simulation of a steady-state electron shock wave in a submicrometer semiconductor device*, *IEEE Trans. Electron Devices* **38** (1991) 392–398.
21. A. M. Anile and O. Muscato, *Improved hydrodynamical model for carrier transport in semiconductors*, *Phys. Rev.* **B51** (1995) 16728–16740.
22. S. R. de Groot and P. Mazur, **Nonequilibrium Thermodynamics** (Dover, 1985).
23. C. D. Levermore, *Moment Closure Hierarchies for Kinetic Theories*, *J. Stat. Phys.* **83** (1996) 331–407.
24. C. Truesdell and R. G. Muncaster, **Fundamentals of Maxwell's Kinetic Theory of a Simple Monoatomic Gas** (Academic Press, 1980).
25. R. LeVeque, **Numerical Methods for Conservation Laws** (Birkhäuser, 1990).
26. B. Van Leer, *Towards the ultimate conservative difference scheme V. A second-order sequel to Godunov's method*, *J. Comput. Phys.* **32** (1979) 101–136.
27. A. Harten and S. Osher, *Uniformily high-order accurate non-oscillatory schemes*, *SIAM J. Numer. Anal.* **24** (1987) 279–309.
28. R. E. Caflisch, G. Russo and Shi Jin, *Uniformly accurate schemes for hyperbolic systems with relaxation*, *SIAM J. Numer. Anal.* **34** (1) (1997) 246–281.
29. F. Liotta, V. Romano and G. Russo, *Central schemes for system of balance laws*, *Internat. Series Numer. Math.* **130** (1999) 651–660.
30. T. Vogelsang and W. Haensch, *A novel approach for including band structure effects in a Monte Carlo simulation of electron transport in silicon*, *J. Appl. Phys.* **70** (1991) 1493–1499.
31. A. Gnudi, F. Odeh and M. Rudan, *Investigation of non-local transport phenomena in small semiconductor devices*, *Euro. J. Telecom.* **1** (1990) 307–312.